# COMPARISON OF ACOUSTIC DOPPLER AND PARTICLE IMAGE VELOCIMETRY CHARACTERIZATIONS OF A CROSS-FLOW TURBINE WAKE

**Benjamin Strom, Steven L. Brunton, Alberto Aliseda, and Brian Polagye[1]**
Northwest National Marine Renewable Energy Center
University of Washington
Seattle, WA, USA

[1]Corresponding author: bpolagye@uw.edu

## INTRODUCTION

Engineering experience with axial-flow wind and water turbines suggests that when streamwise turbine spacing is less than ten diameters, the wake from upstream turbines significantly degrades the power output of downstream turbines and imposes higher fatigue loads (e.g., [1]). It has been hypothesized that cross-flow turbines may be able to achieve higher array efficiencies than axial-flow turbines, particularly in situations where dense arrays are desirable [2, 3]). Cross-flow turbines can also obviate the need for yaw control and can be arranged in high blockage configurations to enhance power output [4].

In dense arrays, power output may be increased when the turbines are controlled in a coordinated manner, allowing downstream turbines to beneficially interact with the flow structures produced by upstream turbines [2, 3]. This type of coordinated control may benefit from reduced order models that describe the wake within the array from a limited set of online measurements (e.g., the angular position, velocity, and acceleration of each turbine). The construction of such models does, however, require a thorough understanding of cross-flow turbine wakes. There have been a number of recent studies in this area, including a study of a hydrokinetic turbine by Bachant and Wosnik [5], which characterized the time-average wake at a vertical plane one turbine downstream. Given the complicated, unsteady flow dynamics present in normal operation of cross-flow turbines (e.g., [6]), an improved understanding is best gained experimentally.

## METHODS

The objective of these experiments was to apply two classes of experimental techniques to characterize the time-average and phase-average wake in close proximity to a cross-flow turbine. The first method is acoustic Doppler velocimetry (ADV), where the Doppler shift in an acoustic pulse is used to characterize three-dimensional velocity over a small, cylindrical volume of water. This is, essentially, a point measurement. The second method is particle image velocimetry (PIV), where a laser sheet is used to periodically illuminate a plane in the flow. By comparing scattered light patterns between two images collected during closely separated illumination periods, the two components of in-plane velocity can be computed throughout the domain. For both techniques, measurements focused on three horizontal planes: the turbine mid-plane (50% blade span), near the top (10% blade span), and near the bottom (90% blade span). The upstream edge of the measurement planes were located one turbine diameter downstream from the axis of rotation. The measurement planes were two diameters in each dimension and centered on the axis of rotation.

### Experimental Facility

Experiments were conducted in a flume at the Bamfield Marine Science Centre (BMSC) in Bamfield, Canada. The flume is 0.98 m wide, has a 10 m long working section, and was operated at a depth of 0.78 m. During experiments, the ratio of turbine and test rig cross-sectional area to flume cross-sectional area was 7%, such that blockage effects should be minimal. Mean current velocity was maintained at 0.8 m/s and turbulence intensity was 4%. The flume was equipped with a chiller that maintained the water temperature at 15 $^{o}$C for the duration of the experiments.

**Experimental Turbine**

Properties of the experimental turbine are given in Table 1 and the experimental setup is shown in Figure 1. The blades of the experimental turbine had a relatively large chord length to maximize the size of the leading edge vortices shed from the blade and increase the potential for detection of these coherent structures by ADV and PIV. This resulted in a turbine that is at the upper end of solidities expected for commercial scale turbines. During experiments, the turbine was operated at constant rotation rate by a servomotor equipped with a high-resolution position encoder. Turbine hydrodynamic torque was transferred by a central drive shaft coupled to a servomotor on the upper end and supported by a low-friction bearing on a vacuum plate on the lower end. Loads and torques were measured on both ends by 6-axis load cells. During testing, the Reynolds number was 4.2x10$^4$, as characterized by the chord length and undisturbed free-stream velocity. The turbine was operated at its peak efficiency (25%), corresponding to a tip-speed ratio of 1.15.

**TABLE 1. EXPERIMENTAL TURBINE PROPERTIES.**

| Parameter | Value |
|---|---|
| Blade profile | NACA 0018 |
| Mount point | ¼ chord |
| Blade pitch angle | 6$^{o}$ |
| Blade helix angle | 0$^{o}$ (straight blades) |
| Number of blades ($N$) | 2 |
| Blade length ($L$) | 23.4 cm |
| Turbine diameter ($D$) | 17.2 cm |
| Chord length ($c$) | 6.1 cm |
| Blade connection | Circular caps at ends of blade span |
| Chord to radius ratio ($c/r$) | 0.71 |
| Solidity ($Nc/\pi D$) | 0.45 |

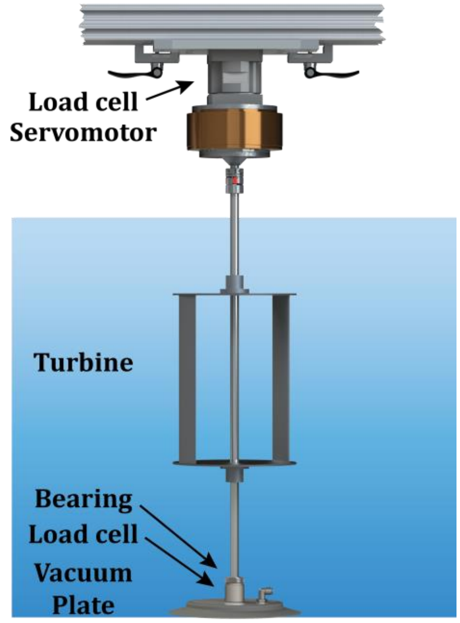


**FIGURE 1. EXPERIMENTAL SETUP.**

**Acoustic Doppler Velocimetery**

ADV measurements were obtained by two Nortek Vectrino Profilers sampling at 100 Hz. The instruments were synchronized with turbine performance measurements, such that the angular position of the turbine was known for each velocity sample. The instruments were attached to an x-y-z traverse system that allowed them to be repeatably positioned at desired locations in the flow. To minimize the hydrodynamic interference due to the instrument presence, the support for the sensor head was faired with a NACA 0015 cross-section. The instruments sampled the flow for 30 s at each equally-spaced position within the measurement plane (2$D$ x 2$D$), with 1 cm resolution (0.06$D$) spacing between measurement locations. The use of two instruments reduced the time required to complete the measurements by a factor of two, but each horizontal plane still required approximately 9 hours of acquisition time.

Acquired data were de-spiked using the method of Goring and Nikora [7]. Data points with a poor signal-to-noise ratio were discarded. In addition to time-average quantities, data were phase-averaged over 6$^{o}$ arcs (30 segments describing 180$^{o}$ of rotation). Regularized results are presented for the along-channel component ($u$), across-channel component ($v$), and vertical component ($w$), and horizontal velocity ($U$, vector mean of $u$ and $v$).

**Particle Image Velocimetry**

PIV measurements were obtained from a single-camera LaVision system owned by the Bamfield Marine Science Centre. The camera field of view was approximately 18 cm x 22 cm, requiring four measurement planes to cover the $2D$ x $2D$ downstream region. Camera resolution was 1024 x 1344 pixels. Naturally occurring particles were used as PIV-seed scatterers. Collection of image pairs was phase-locked to the turbine azimuthal position using a Matlab Simulink model running on the Windows realtime kernel. One hundred image pairs were collected for each angular blade position from zero to 180 degrees (a half revolution due to the axisymmetric turbine geometry) in increments of six degrees. The time interval between image pairs was 1 ms, corresponding to a displacement of ~5 pixels at the free stream velocity. Images were post-processed by a global contrast filter. Vector fields were then computed for image pairs and registered to Cartesian space using a linear transformation obtained from images of a calibration target in the measurement plane (2.5 mm white circles on a 1 cm grid). The vector fields were then processed by signal-to-noise filter, peak height filter, global outlier filter, and two sizes of local median filters. Vector fields for each blade position were averaged to return the phase-average field corresponding to a given angular position of the turbine.

## RESULTS

ADV measurements of mean velocities for the three planes are shown in Figure 2. The mean horizontal velocity and along-channel velocity components measured by ADV and PIV are generally comparable, while the observed across-channel velocity is more intense for ADV than PIV (not shown). Similar to Bachant and Wosnik [5], large across-channel ($y$-direction) variations and asymmetry are observed, though the asymmetry is greater in the present experiments, possibly as a consequence of a higher $c/R$ and solidity. Significant vertical variation is observed for all components of velocity, but there is limited vertical asymmetry.

The progression of the phase-average wake evolution is shown in Figure 3 for mid-plane measurements. The overall trends are qualitatively similar, but ADV resolves a strong, coherent vortex pair, which is less evident in the PIV measurement. The reason for this is apparent when one considers the phase-average vertical velocity measured by the ADV. Near the vortex pair, the vertical velocity is sufficient for the particles in this region to traverse the laser plane in the time interval between images. Thus, these regions are not observable in the PIV measurements using a thin laser sheet.

## DISCUSSION

### Opportunities for Coordinated Control

The wake structure has notable implications for the operation of dense arrays with coordinated control. First, as is the case for any bluff body, the along-channel velocity ($U$) is intensified by the presence of the turbine, exceeding the upstream magnitude in some regions of the wake. A turbine positioned in a region of elevated along-channel velocity, but outside of the strongest shear, may be able to harness this localized increase in kinetic power. However, the leading edge vortices shed by the turbine pass through this region (coherent structure observed from $90^{\circ} < \theta < 150^{\circ}$ in Figure 3). A downstream turbine operating in this region would likely need to coordinate the phase of its blades in their power strokes with the passage of these vortices.

### Relative Effectiveness of ADV and PIV

While ADV measurements were time-intensive to perform, the technique produced superior information to PIV during this set of experiments. Future experiments, using a new system at the University of Washington, are likely to shift this balance in favor of PIV. The new system will enable stereoscopic, time-resolved PIV measurements of the turbine wake over an image plane approximately four times larger than at BMSC. In addition, the stereoscopic system will eliminate the need for a thin laser sheet, and thus regions of high vertical velocity will be fully resolved.

## CONCLUSIONS

Time-average and phase-average measurements of a cross-flow turbine reveal wake structures that may be used for coordinated control. Time-average ADV and PIV measurements of the wake are in general agreement. Phase-average ADV measurements are more successful in resolving the primary coherent structure due to the ejection of particles from the PIV measurement plane between image pairs by the localized pockets of strong vertical velocity. Future work will involve the development of a reduced order model for the cross-flow turbine wake to enable coordinated array control.

## ACKNOWLEDGEMENTS

Funding for these experiments was provided by the US Department of Energy under the Advanced Laboratory and Field Arrays project (DE-EE0006816). Support for the construction of the experimental test rig and ADV traverse system was provided by the US Department of Defense Naval Facilities Engineering Command (NAVFAC).

Many thanks to the Bamfield Marine Science Centre for hosting the experiments and, especially Eric Clelland for his assistance with the PIV measurements.

**REFERENCES**


[1] Vermeer, L. J., Sørensen, J. N., & Crespo, A., 2003, Wind turbine wake aerodynamics. *Progress in Aerospace Sciences*, 39(6), 467-510.

[2] Dabiri, J. O., 2011, Potential order-of-magnitude enhancement of wind farm power density via counter-rotating vertical-axis wind turbine arrays. *Journal of Renewable and Sustainable Energy*, 3(4), 043104.

[3] Dabiri, J. O., 2010, Fish schooling as a basis for vertical-axis wind turbine farm design. *Bioinspiration and Biomimnetics* 5:035005

[4] Garrett, C., & Cummins, P., 2007, The efficiency of a turbine in a tidal channel. *Journal of Fluid Mechanics*, 588, 243-251.

[5] Bachant, P. and Wosnik, M., 2015. Characterising the near-wake of a cross-flow turbine. *Journal of Turbulence*, 16(4), pp.392-410.

[6] Dunne, R. and McKeon, B.J., 2015. Dynamic stall on a pitching and surging airfoil. *Experiments in Fluids*, 56(8), pp.1-15.

[7] Goring, D. G., & Nikora, V. I., 2002, Despiking acoustic Doppler velocimeter data. *Journal of Hydraulic Engineering*, 128(1), 117-126.


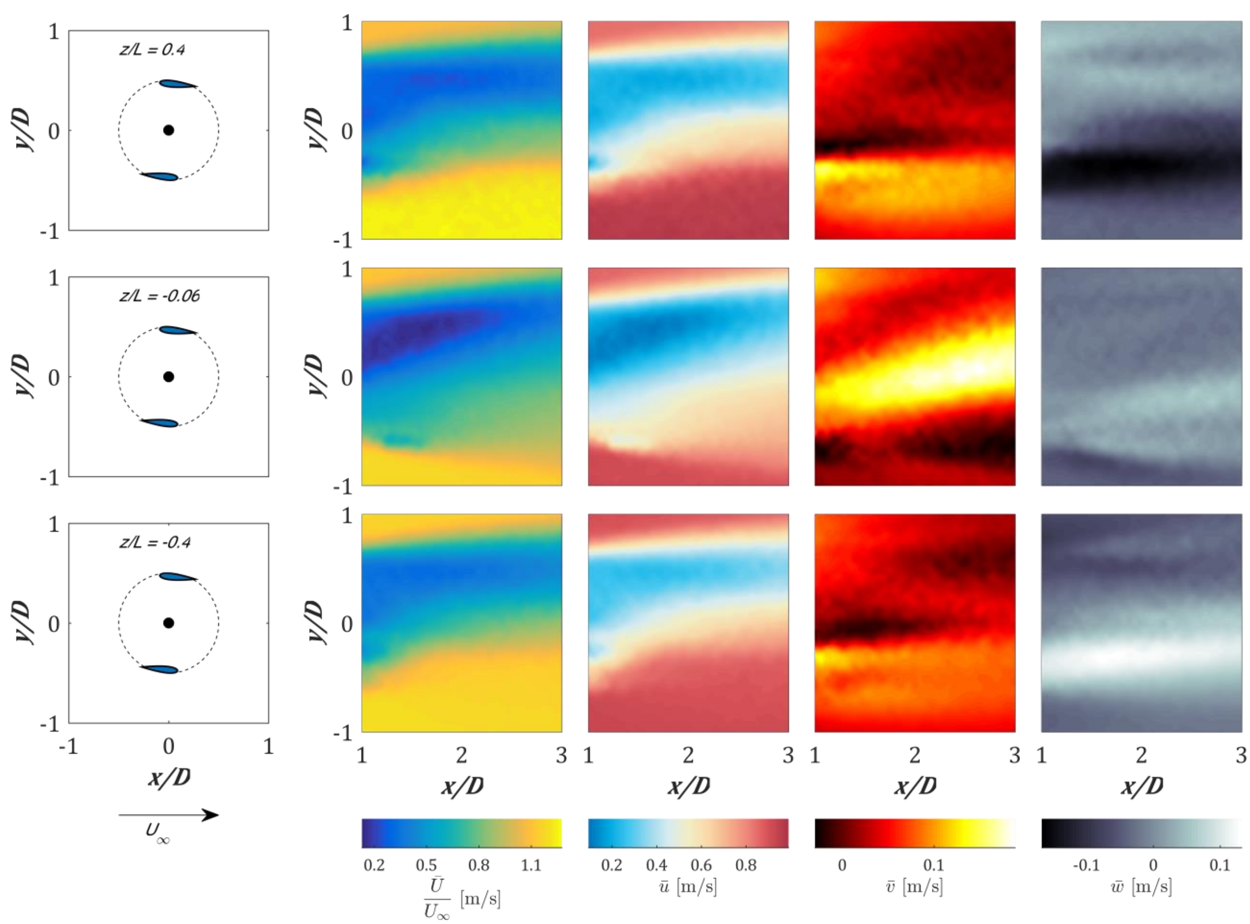


**FIGURE 2. TIME AVERAGE TURBINE WAKE FROM ADV MEASUREMENTS**

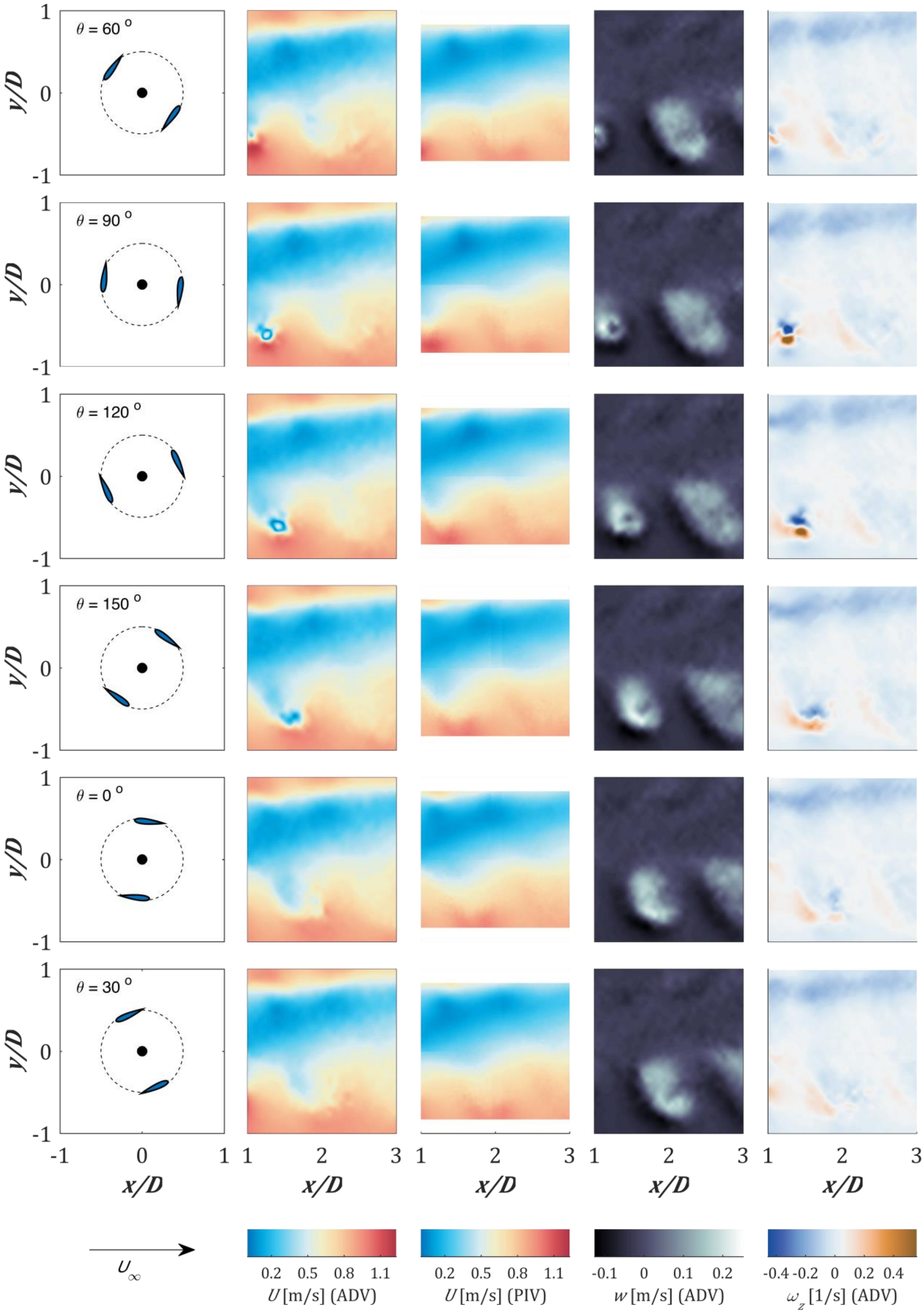


**FIGURE 3. PHASE-AVERAGED TURBINE WAKE FROM ADV AND PIV MEASUREMENTS AT THE TURBINE MID-PLANE. THE SHED VORTEX PAIR LOCATION IS IDENTIFIED BY REGIONS OF HIGH VORTICITY (RIGHT COLUMN).**